Radiation Properties of Carbon Nanotubes Antenna at Terahertz/Infrared Range

Article *in* International Journal of Infrared and Millimeter Waves · January 2008

DOI: 10.1007/s10762-007-9306-9

6 authors, including:

Yue Wang
Xi'an University of Technology
71 PUBLICATIONS **544** CITATIONS

SEE PROFILE

Int J Infrared Milli Waves (2008) 29:35–42
DOI 10.1007/s10762-007-9306-9

Radiation Properties of Carbon Nanotubes Antenna at Terahertz/Infrared Range

Yue Wang · Qun Wu · Wei Shi · Xunjun He · Xiaofang Sun · Tailong Gui

Abstract The geometric structure and the terahertz/infrared radiation characteristics of carbon nanotubes dipole antenna arrays have been investigated by CST MICROWAVE STUDIO based on finite integral methods. In terahertz and infrared frequency span, the antenna properties such as electrical field distributions, scattering parameters, standing wave ratio, gain, and two dimension directivity patterns are discussed. Our results show that $N \times N$ antenna arrays have higher radiation efficiency than single carbon nanotube dipole antenna.

Keywords Carbon nanotube · Terahertz/infrared · Antenna arrays

1 Introduction

Carbon nanotubes (CNTs) have been of great interest for use as electronic devices such as field emission sources [1], transistors [2] and nanotransmission lines [3] because of the outstanding metallic conductivity and mobility along the entire length. Since the discovery of the unique antenna from CNTs in 2004 [4], there has been more strong interest in nano-antenna, and much concerning their length from nanometer scale to centimeters [5, 6], naturally, which leads to a topic considering CNTs for sub-millimeter, millimeter and centimeter wave antenna applications. At the same time, vertically-aligned CNTs grown successfully by several research groups [7, 8] are extremely attractive for possible practical

This work was supported by National Natural Science Foundation of China (60571026, 10396160).

Y. Wang (✉) · X. He · T. Gui
Harbin University of Science and Technology, Harbin 150080, People's Republic of China
e-mail: wsbte@126.com

Q. Wu
Harbin Institute of Technology, Harbin 150001, People's Republic of China

Y. Wang · W. Shi · X. Sun
Xi'an University of Technology, Xi'an 710048, People's Republic of China

applications of CNTs in THz nano-antenna and other nanoelectronic devices to connect with macroscopic outside world.

In recent years, there are two methods to generate THz radiation. In the first method, called optical rectification, frequency components in the bandwidth of an ultrashort laser pulse are mixed in a nonlinear crystal such as ZnTe or GaP, to generate a few-cycle THz pulse [9–11]. In the second, called photoconductive switching, an ultrashort laser pulse illuminates a semiconductor such as GaAs, biased with an electric or a magnetic field, giving rise to an ultrafast current transient which emits a THz pulse. But the disadvantage of methods above is that the peak electric fields of THz wave are generally much smaller than that generated by the biased emitters. An alternative method is the nano-antennas, which typically have dimensions from several microns to several tens of microns. Generally, the detection methods of THz radiation include bolometer [12] with detectors, electro-optic detection in a crystal [13] and micro-fabricated antenna on low-temperature semiconductors or radiation damaged Si on sapphire substrate [14]. However, bolometer operation needs to be cooled by liquid helium, electro-optic detection has the disadvantage of multiple reflections and reshaping of the THz pulse due to phase matching issue lending to distorted THz radiation, and micro-fabricated antenna requires specific expertise to make them using clean room facilities.

In order to reduce the disadvantages about THz systems mentioned above, a novel THz generation/detection method based on nanotubes antenna has been presented here. It is appropriate to consider their possible use as THz nano-antennas. At the same time, an effective circuit model for the ac high-frequency electronic properties of carbon nanotubes has recently been proposed in [3]. The high frequency circuit model developed may have direct applications in determining the switching speed of a variety of nanotubes based electronic devices.

However, one of the most important unsolved problems in nanotechnology is how to make electrical contact from nanoelectronic devices to microscopic electronic devices. Based on this idea, the purpose of the present study is to simulate and optimize a computing structure model for electric field analysis and to discuss the important parameters such as field distribution, gain, radiation direction patterns and radiation efficiency of simple dipole antenna system based on CNTs. As long as a proper computing model and a computer simulation method are proposed, then computer simulation of far field analysis for vertically-aligned CNTs antenna becomes possible, and we can make clear that far field radiation characteristics can be obtained from vertically-aligned CNTs dipole antennas.

2 Computing model and structure description

A carbon nanotube consists chemically of a sheet of graphite rolled up into a tube. The structure of the nanometric antenna element and its corresponding coordinates are shown in Fig. 1 (a). The geometry structure can be modeled by a suitable combination of two surfaces, such as cylindrical surface as a tube part and half hemispherical surface as a cap part. In order to provide room for the location of the excitation source, a small gap, that is, feeding ports modeled by round plane surfaces is cut in the antenna afterwards and the gap between two ports is d. The diameter and the total length of the antenna are R and L. The total length of the structure is $L=\lambda/2$, where λ is the wavelength. Thus, one electric dipole is modeled by means of a single very thin cylinder composed of the perfect electric conductive (PEC) material. Since the array pattern consists of identical elements, the single dipole is then multiplied to obtain the final structure. Figure 1(b) displays the side-view of

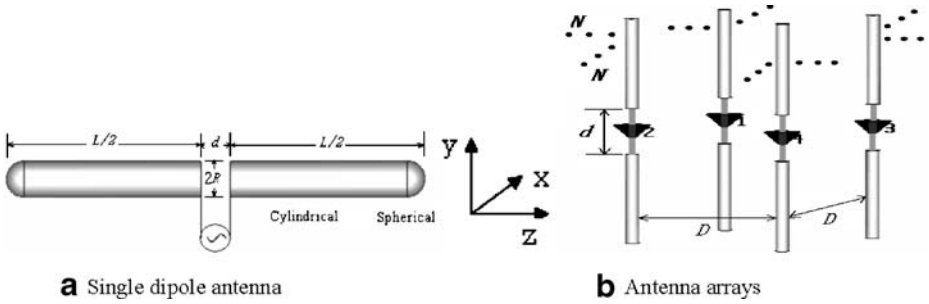

Fig. 1 Dipole antenna structure model for the CNT. (**a**) Single dipole antenna element and corresponding coordinates. (**b**) $N \times N$ antenna arrays, where the intertube distance is D.

the configuration of the antenna $N \times N$ array pattern consisting of $N \times N$ identical single electric dipoles, each holding a length of λ/2. Taking advantage of the given symmetry of the structure, one corresponding symmetry plane is defined.

Since the structures are very small PEC elements, it is necessary to refine the mesh in order to obtain results of sufficient accuracy. Therefore, both the number of mesh density per wavelength and the refinement factor at conductor edges are increased. As a result, the numbers of meshnodes are increased.

3 Antenna design and result analysis

3.1 The radiation properties of 1 μm CNTs antenna in the different inputting frequency

For computer simulation of radiation characteristics of carbon nanotubes (CNTs) by means of CST, we assume that CNTs are PEC materials. The average density of CNTs is typically as large as 10^9 /cm^2. Exact modeling of such a large number of CNTs is practically impossible. In our simulation, therefore, CNTs antennas are modeled by $N \times N$ CNTs array elements.

We first treat a rather ideal case, that is, a 2×2 CNTs antenna array which consists of hemispherical-capped CNTs having a uniform length. In practical CNTs systems, however, the CNTs lengths are different from each other. The geometric parameters of CNTs array

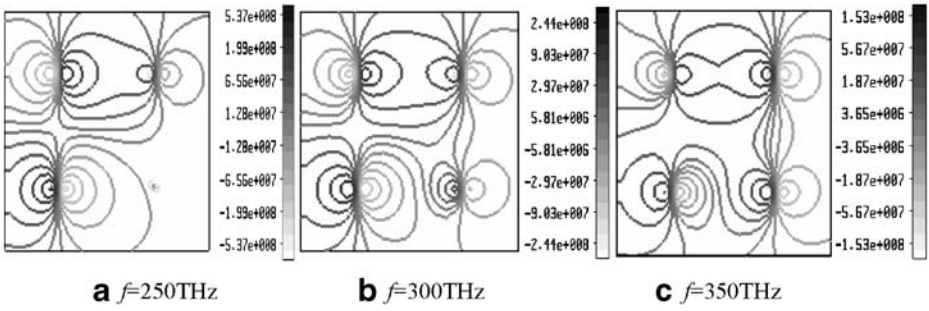

Fig. 2 The distribution of electric field isolines at the CNTs apex on *z*-*x* plane for different values of frequency.

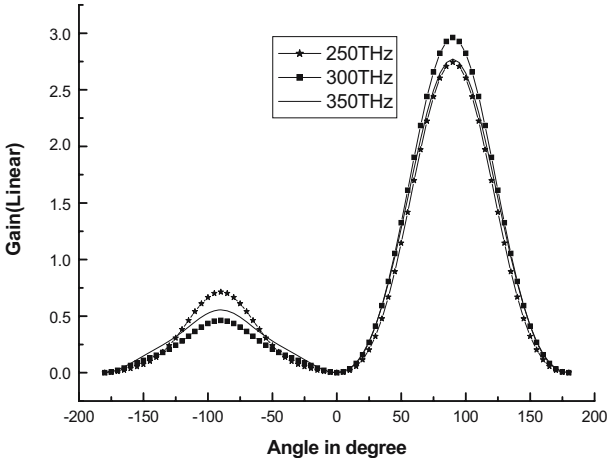

Fig. 3 Gain of half wave dipole antenna arrays.

used for simulation are listed as follows: λ=1000 *nm*, *L*=0.48 λ, *R*=0.01λ, and *d*=0.1λ. The distance of both dipole antenna elements is *D*=λ/4.

The resonant frequency is related to the electrical length of the antenna. The electrical length is usually the physical length of the wire multiplied by the ratio of the speed of wave propagation in the wire. Typically an antenna is tuned for a specific frequency, and is effective for a range of frequencies usually centered on the resonant frequency. However, other properties of the antenna (especially radiation pattern and impedance) change with frequency, so the antenna's resonant frequency may merely be close to the center frequency. In the following section, the distribution of electric field and radiation pattern of CNTs antennas for different values of frequency have been investigated.

Figure 2 shows a typical example of simulation for electric field isolines in the end parts of CNTs arrays under the condition of gradually increased frequency (from left to right), *i.e.*250THz, 300THz and 350THz. It is clear that the electric field strength at the CNTs apex greatly decreases with the increasing frequency.

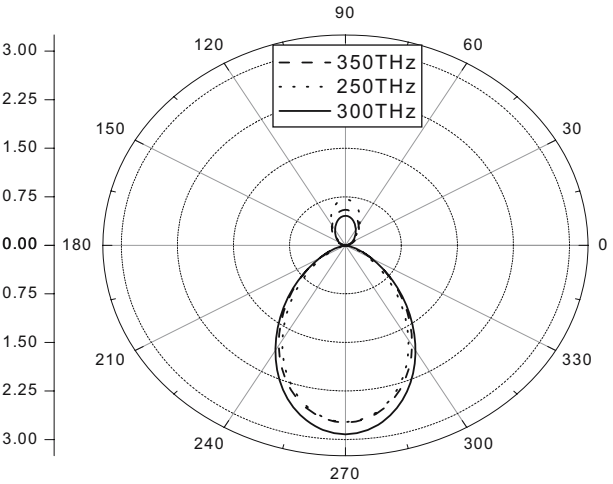

Fig. 4 Directivity pattern of CNTs antenna arrays.

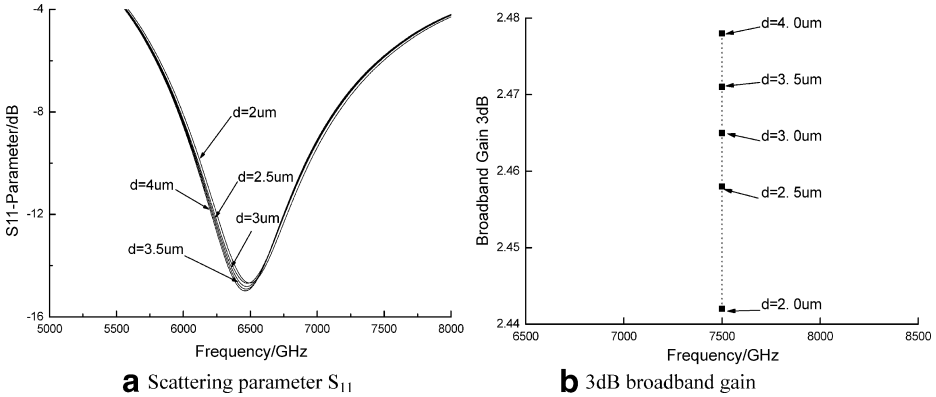

Fig. 5 Radiation properties of CNTs antenna (L=20 μm, R=2.712). (**a**) S_{11} dependent frequency of CNTs antenna with varying gap widths. (**b**) 3dB broadband gain dependent frequency of CNTs antenna with varying gap widths.

In antenna design, gain is a measure of the ability of the antenna to direct the input power into radiation in a particular direction and is measured at the peak radiation intensity. Figure 3 shows the gain of dipole antenna arrays under the condition of different frequencies. From these results it can be seen that, unlike classical metal dipole antennas, the gain of CNTs dipoles is very low due to their extremely small radius. The linear gain of the antenna arrays is 2.77, 2.96 and 2.74, corresponding to the frequency of 350THz, 300THz and 250THz, respectively. In general, the higher the frequency, the higher the gain. But the possible oscillating behavior of CNTs in high frequency and the influence of array elements each other lead to a larger degradation of gain at higher frequencies. From Fig. 4, directivity patterns of CNTs antenna arrays illustrate the same problem, and shows that the difference of main lobs magnitude of array changes with the different frequency.

3.2 The radiation properties of CNTs antenna under the condition of different *d*s and *D*s

In this section, the armchair metal CNTs (m=n=40) are simulated for the case of different $N \times N$ array elements. The scattering parameter S_{11}, voltage standing wave ratio (VSWR), gain and directivity parameters of different CNTs antenna arrays have been investigated for 5×5, 9×9, 15×15 and 25×25 arrays.

Table 1 Typical geometric parameters and antenna arrays parameters in different intertube distances.

Parameters	Array	Distance(D)	Gain(Line)	Main Lobes Magnitude	Reference Column
f=10THz λ=30 μm	5×5	λ/17*	5.374	3.22	*Good directivity
L=0.485λ		λ/30	4.0	2.93	Including side lobe
R=2.712 nm	9×9	λ/10	9.285	4.5	Including side lobe
d=0.015λ (Meshcell:		λ/30*	5.916	3.289	*Good directivity
10044, Factor:10)	15×15	λ/30	6.698	2.0	Including side lobe
		λ/50*	7.079	3.496	*Good directivity
	25×25	λ/30	7.379	3.88	Including side lobe
		λ/80*	6.425	3.307	*Good directivity

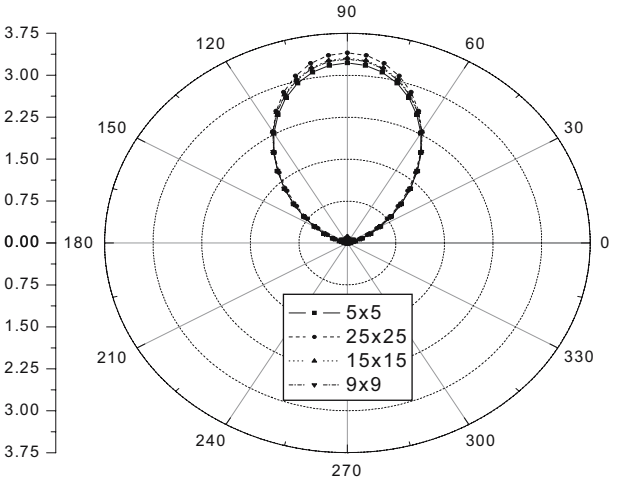

Fig. 6 Two dimensional antenna directivity patterns of four arrays of dipole elements with different distance of *D*.

In Fig. 5 (a), the scattering parameter S_{11} of a CNTs dipole holding half wavelength L=20 μm (λ=40 μm) and R=2.712 *nm* for five gradually increased gap width (d from 2 μm to 4 μm) is shown. From this, we can find that S_{11} almost does not change with width *d*. The 3dB broadband gain in Fig. 5 (b) changes from 2.442dB to 2.478dB, corresponding to the gap width changing from 2 μm to 4 μm. For the case of L=30 μm (f=5THz), the same result is obtained.

In Fig. 5 (a), noticeably, the resonant frequency is in disagreement with the electrical length. In general, the length of a dipole is the main determining factor for the operating frequency of the dipole antenna. Although the antenna may be of an electrical half wavelength, or multiple of half wavelengths, it is not exactly of the same length as of the wavelength for a signal traveling in free space. There are a number of reasons for this, which means that an antenna will be slightly shorter than the length calculated for a wave traveling in free space.

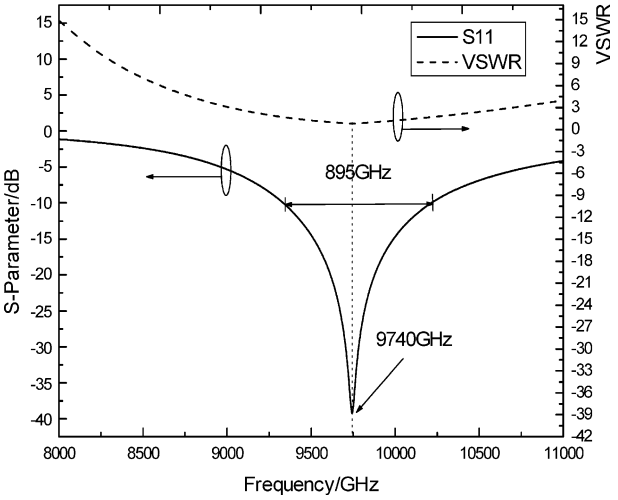

Fig. 7 S-parameter and VSWR vs. Frequency.

Typical examples of CNTs antenna geometric parameters and all kinds of other parameters are shown in Table 1, where the total number of meshcells is 10044, and the refinement factor is 10. The meshcell density and refinement factor are very important for determining the accuracy in the parameter calculation. In order to provide a comparison for different $N \times N$ antenna arrays, which corresponds to the condition of different intertube distances, it would be useful to make fixed structure parameters. The details of antenna parameters with the intertube distance (D) are given in Table 1. Figure 6 shows that CNTs antenna arrays have remarkable directivity labeled by symbol * in Table 1.

Figure 7 below shows the S-parameters and VSWR as a function of frequency, where the resonant frequency (9.7THz) is less than the practical electrical length calculated, and VSWR is less than 2.0 under the operating frequency from 9.34THz to 10.24THz.

4 Conclusion

The geometric structure simulation and the THz/infrared radiation properties of nanometric antenna arrays have been studied by the CST MICROWAVE STUDIO based on the finite integral method. Both the numerical and analytical results demonstrate that the antenna holding half wave length of 15 μm takes on the resonance frequency properties from 9.34THz to 10.24THz in the center frequency of 9.74THz corresponding −10dB return loss bandwidths of 9.1%, and that VSWR is less than 2.0 in this frequency range. Although the single dipole element exhibits very low gain and efficiency, we can possibly improve the antenna gain by controlling the length, intertube distance, and the number of nanotube elements. The maximum linear gain of typical 15×15 CNTs antenna arrays is 7.079, main lobe magnitude and direction is 3.496, 90 degrees respectively. These simulation methods and results can be used in the design of optimal emitters/receivers to generate/receive high-energy THz pulse trains for applications in communications, nonlinear optics, and coherent control, or infrared detection.

Acknowledgment The work performed by Q. Wu was partially supported by the National Natural Science Foundation of China (60571026), and work by W. Shi was partially supported by the National Natural Science Foundation of China (10396160).

References

1. W. A. de Heer, A. Châtelain and D. Ugarte, A carbon nanotube field-emission electron source, Science **270**, 1179–1180 (1995).
2. S. Li, Z. Yu, and S. F. Yen, *et al.*, Carbon nanotube transistor operation at 2.6 GHz, Nano Lett. **4**, 753–756 (2004).
3. P. J. Burke, An RF circuit model for carbon nanotubes, IEEE Trans. Nanotechnol. **2**, 55–58 (March 2003).
4. Y. Wang, K. Kempa, B. Kimball, *et al*., Receiving and transmitting light-like radio waves: Antenna effect in arrays of aligned carbon nanotubes, Appl. Phys. Lett. **85**(13), 2607–2609 (2004).
5. S. D. Li, Zhen Yu, and C. Rutherglen, *et al.*, Electrical Properties of 0.4 cm Long Single Walled Carbon Nanotubes, *Nano Lett*. **4**(10), 2003–2007 (2004).
6. A. Javey, P. F. Qi, Q. Wang, *et al*., Ten- to 50-*nm*-long quasi-ballistic carbon nanotube devices obtained without complex lithography, PNAS. **101**(37), 13408–13410 (2004).
7. M. Kusunoki, T. Suzuki, and K. Kaneko, *et al*., Formation of self-aligned carbon nanotube films by surface decomposition of silicon carbide, Phil. Mag. Lett. **79**, 153–161 (1999).
8. H. Murakami, M. Hirakawa, C. Tanaka and H. Yamakawa, Field emission from well-aligned, patterned, carbon nanotube emitters, Appl. Phys. Lett. **76**, 1776–1778 (2000).
9. X. C. Zhang, Y. Jin and X. F. Ma, Coherent measurement of THz optical rectification from electro_optic crystals, Appl. Phys. Lett. **61**, 2764–2766 (1992).

10. A. Nahata, A. S. Weling, and T. F. Heinz, A wide band coherent terahertz spectroscopy system using optical rectification and electro-optic sampling, Appl. Phys. Lett. **69**, 2321–2323 (1996).
11. A. Bonvalet, M. Joffre, and J. L. Martin, *et al.*,Generation of ultrabroadband femtosecond pulses in the mid-infrared by optical rectification of 15 fs light pulses at 100 MHz repetition rate, Appl. Phys. Lett. **67**, 2907–2909 (1995).
12. B. I. Greene, J. F. Federici, and D. R. Dykaar, *et al.*, Interferometric characterization of 160 fs far-infrared light pulses, Appl. Phys. Lett. **59**(8), 893–895 (1991).
13. Q. Wu and X.-C. Zhang, Ultrafast electro-optic field sensors, Appl. Phys. Lett. **68**(12), 1604–1606 (1996).
14. Y. Cai, I. Brener, and J. Lopata, *et al.*, Coherent Terahertz Radiation Detection: Direct Comparison between Free-Space Electro-optic Sampling and Antenna Detection, Appl. Phys. Lett. **73**(4), 444–446, (1998).